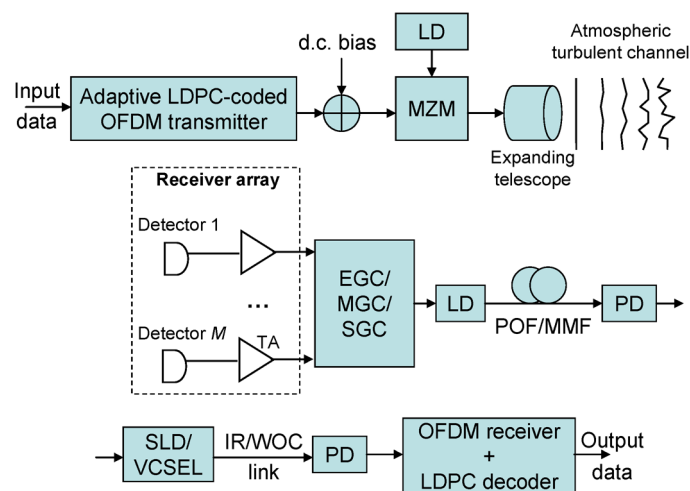


# LDPC-Coded OFDM for Heterogeneous Access Optical Networks

Volume 2, Number 4, August 2010

Ivan B. Djordjevic, Member, IEEE  
Hussam G. Batshon, Student Member, IEEE



DOI: 10.1109/JPHOT.2010.2051943  
1943-0655/\$26.00 ©2010 IEEE

# LDPC-Coded OFDM for Heterogeneous Access Optical Networks

Ivan B. Djordjevic, *Member, IEEE*, and  
Hussam G. Batshon, *Student Member, IEEE*

Department of Electrical and Computer Engineering, University of Arizona, Tucson, AZ 85721 USA

DOI: 10.1109/JPHOT.2010.2051943  
1943-0655/\$26.00 ©2010 IEEE

Manuscript received May 5, 2010; revised May 27, 2010; accepted May 27, 2010. Date of publication May 28, 2010; date of current version June 22, 2010. This work was supported in part the National Science Foundation under the Integrative, Hybrid, and Complex Systems Grant 0725405. Corresponding author: I. B. Djordjevic (e-mail: ivan@ece.arizona.edu).

**Abstract:** In this paper, we propose a heterogeneous optical access networking scenario, in which communication links between source and destination nodes are heterogeneous, composed of free-space optical, plastic optical fiber (POF), and indoor infrared (IR) links. To deal with bandwidth limitations of POF and IR links, a power-variable rate-adaptive low-density parity-check (LDPC)-coded orthogonal frequency division multiplexing (OFDM) scheme is used, while to deal with atmospheric turbulence, the spatial diversity is used. The rate-adaptive LDPC codes are designed using a modified progressive edge-growth (MPEG) algorithm. We show that with the proposed heterogeneous communication systems, we can deliver a high-speed optical signal (40 Gb/s and beyond) to an end-user.

**Index Terms:** Heterogeneous optical networking, access networks, orthogonal frequency division multiplexing (OFDM), low-density parity-check (LDPC) codes, rate-adaptive coding, adaptive power loading.

## 1. Introduction

Internet traffic has continued its rapid growth over the last few years due to the increased popularity of the Internet. Other major contributors to this growth are the new applications that are emerging and continuing the demand for higher bandwidths [1], such as voice over internet protocol (VoIP), YouTube, internet protocol TV (IPTV), and high-definition TV (HDTV). For instance, a single uncompressed HDTV stream (1080i) requires a data rate of about 1.5 Gb/s [2]. Such data rates are too high for conventional wireless LAN systems. This bottleneck can be solved by employing ultra wideband (UWB) communications operating in the 3.1–10.6 GHz range [3] or the more recently proposed 60 GHz radio operating in the 57–64 GHz range (in North America) [2]. Combining transmission of UWB/60 GHz signal over fiber optical links by employing radio-over-fiber (RoF) is a promising technology for extending the coverage of UWB/60 GHz radios. However, this approach requires expensive optical components in addition to frequent electrical-to-optical (E-O) and optical-to-electrical (O-E) conversions. It is also inefficient in terms of optical bandwidth utilization, as it transmits low-speed wireless signals over high-bandwidth optical channel. Another approach to delivering a high-speed signal to an end-user is through the use of passive optical networks (PONs) [4].

In order to reduce the system cost of PONs and speed up the installation process, in this paper, we propose the use of heterogeneous optical networking (HON). The proposed HON can provide high-bandwidth and solve interoperability problems of future optical networks, while keeping the system cost and power consumption reasonably low. With HON, we can deliver a high-speed optical signal, i.e., 40 Gb/s and beyond, to an end-user by using free-space optical (FSO), plastic optical fiber

(POF)/multimode fiber (MMF), and indoor optical wireless communication (OWC) links (also known as infrared (IR) links). The proposed scheme provides solutions to two major obstacles: bandwidth limitation and atmospheric turbulence. To deal with bandwidth limitations of POF/MMF and OWC links we employ power-variable rate-adaptive low-density parity-check (LDPC)-coded orthogonal frequency division multiplexing (OFDM). On the other hand, to deal with atmospheric turbulence we utilize the spatial diversity. The rate-adaptive LDPC codes are designed using modified progressive edge-growth (MPEG) algorithm, initially introduced in [5], which in comparison with quasi-cyclic (QC) LDPC code design [6], [7] offers more flexibility in design of large-girth LDPC codes of shorter length.

This paper is organized as follows. In Section 2, we describe proposed HON scenario and provide several possible applications of interest. In Section 3, we describe the proposed rate-adaptive LDPC code design based on MPEG algorithm and provide BER performance evaluation with respect to previously proposed QC code design. In Section 4, we describe the proposed adaptive MPEG-LDPC-coded OFDM scheme suitable for use in heterogeneous access optical networks and provide aggregate data-rate performance evaluation. Some important concluding remarks are given in Section 5.

## 2. Heterogeneous Optical Networks

Various applications of interest of the proposed HON scenario, which are depicted in Fig. 1, include i) in cellular systems to establish the connection between mobile telephone switching office (MTSO) and base stations (BSs) [see Fig. 1(a)], ii) in WiMAX to extend the coverage and reliability by connecting WiMAX BSs with FSO, hybrid (FSO-RF) or heterogeneous (FSO-POF/MMF) links [see Fig. 1(b)], iii) in UWB communications to extend the wireless coverage range [see Fig. 1(c)], iv) in access networks [Fig. 1(d)] to increase data rate and reduce system cost and deployment time, v) in ground-to-satellite/satellite-to-ground FSO communications to increase the data rate [Fig. 1(e)], vi) in intersatellite FSO communications [Fig. 1(e)], and vii) in aircraft-to-satellite/satellite-to-aircraft communications [Fig. 1(e)].

In order to reduce system installation and maintenance costs for indoor applications, the POFs or MMFs can be used from residential gateway to either fixed or mobile wireless units inside the building. The proposed systems offer many advantages over wireless such as low attenuation loss, large bandwidth, improved security, reduced power consumption, and easy installation and maintenance. The proposed communication system is also an excellent candidate to be used instead of PON applications to substitute various MMF or SMF links as shown in Fig. 1 while reducing system cost and speeding up the installation process. With the FSO link being used as the transmission media, free-space optical access networks (FSO-ANs) can offer much higher bandwidth and better energy efficiency, while supporting various communication services. Instead of optical couplers used in PONs, we can use amplify-and-forward (AF) FSO relays based on semiconductor optical amplifiers, which is illustrated in Fig. 1(d). FSO-ANs have many advantages compared to other conventional copper-based access technologies. For example, FSO-ANs offer an improved bandwidth while supporting various communication services. In combination with OFDM, FSO-ANs have unique flexibility in dealing with bandwidth resource sharing and virtualization, in addition to protocol independence, service transparency, scalability, and cost-effectiveness. Namely, in OFDM based FSO-ANs, we assign to every particular optical network unit (ONU) a subset of subcarriers. This subset of subcarriers can employ different QAM constellation sizes depending on channel signal-to-noise ratio (SNR). Differentiated quality of service (QoS) can easily be achieved by assigning high-quality subcarriers (with high SNR) to higher priority users. Moreover, this OFDM scheme can operate with simple medium access control (MAC) with low overhead.

Fig. 2 shows the block diagram of the proposed heterogeneous optical communication system [one possible link from Fig. 1(d)]. In this setup, the LDPC encoded data enters the buffer in the adaptive OFDM block. Depending on  $i$ th subcarrier SNR,  $m_i$  bits are taken from the buffer. The mapper that follows buffer selects a corresponding constellation point from  $2^{m_i}$ -QAM constellation diagram. After pilot insertion and serial-to-parallel (S/P) conversion, the inverse FFT (IFFT) is performed. The cyclic extension is performed by repeating the  $N_G/2$  samples (of IFFT frame) as a prefix and the first  $N_G/2$  samples as a suffix. The LDPC code of given rate is selected as described

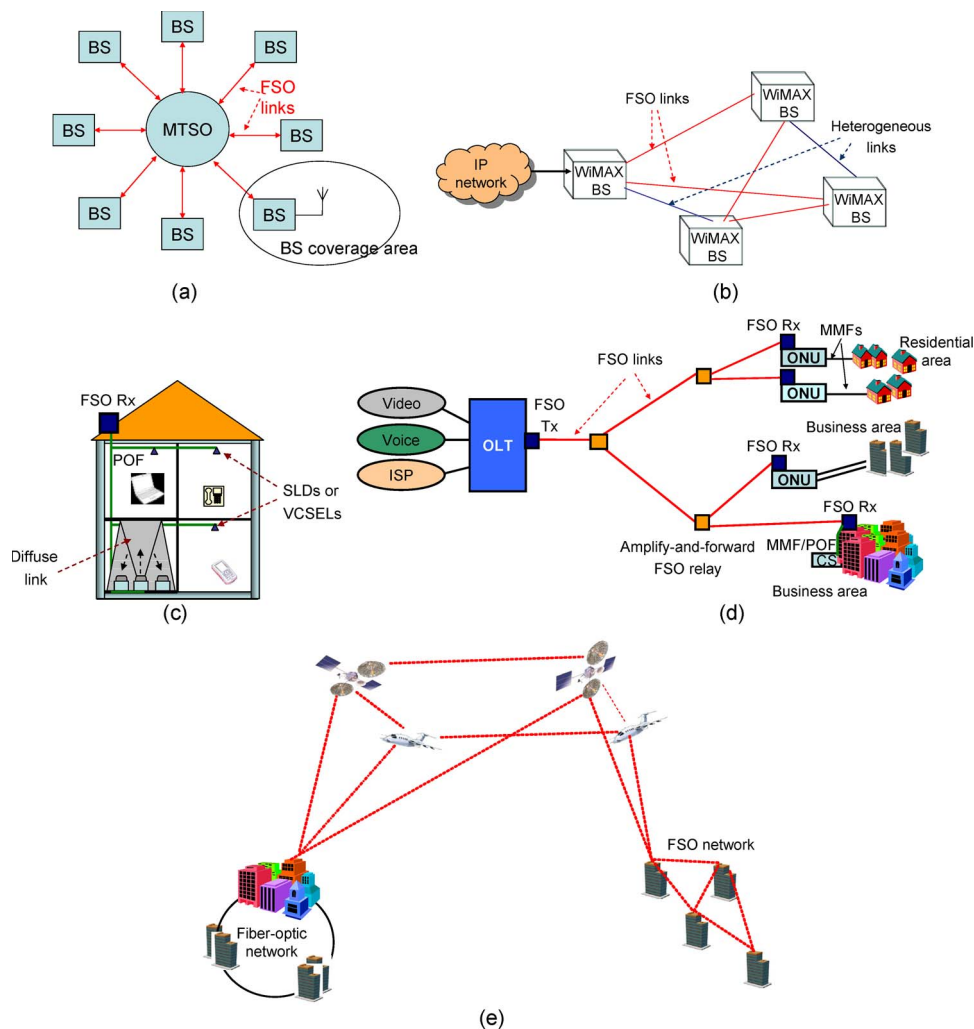


Fig. 1. Heterogeneous optical networking. (a) Cellular network, (b) WiMAX network, (c) indoor optical network, (d) optical access network, and (e) satellite-to-ground/ground-to-satellite, intersatellite, and satellite-to-aircraft/aircraft-to-satellite FSO communications. OLT: optical line terminal, ONU: optical network unit, CS: central station.

in the following section. The dc bias is added so that real-valued OFDM signal can be transmitted over the FSO system with direct detection. The modulated beam is projected toward the distant receiver array by using an expanding telescope assembly. By providing that the aperture diameter of each receiver is smaller than spatial correlation width of irradiance function, the array elements will be sufficiently separated so that they act independently. Possible FSO spatial diversity techniques include equal gain combining (EGC), maximum gain combining (MGC), and selection gain combining (SGC). The signal is then remodulated and transmitted either over MMF or POF. Upon photodetection at the end of MMF/POF link, the signal is retransmitted over an indoor OWC/IR link using either a superluminescent diode (SLD) or a VCSEL. If MMF is used instead of POF, it might be possible to transmit the signal from OLT to an end-user even without any intermediate O-E and E-O conversions.

### 3. Rate-Adaptive MPEG Algorithm Based Large-Girth LDPC Codes

Given this general description of proposed HON, we turn our attention to the design of adaptive LDPC codes using MPEG algorithm. The original PEG algorithm for the design of LDPC( $n, k$ )

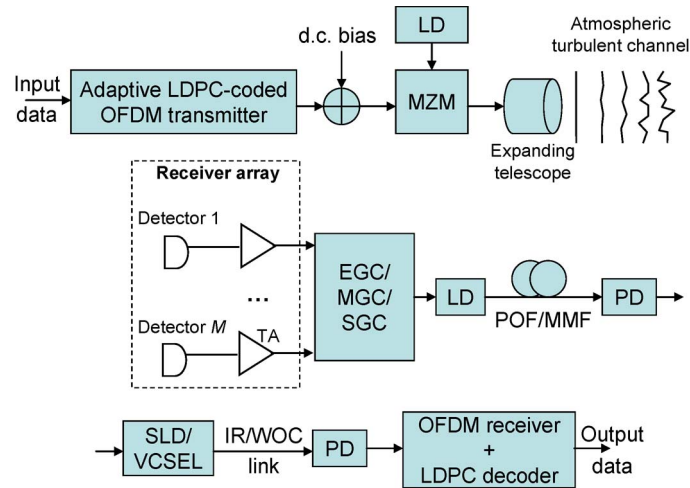


Fig. 2. Block diagram of possible heterogeneous access optical communication systems. LD: laser diode, PD: photodetector, TA: transimpedance amplifier.

codes can be formulated as follows [5]: Given  $(n - k)$ ,  $n$  and variable-node degree distribution, design an  $(n - k) \times n$  parity-check matrix with largest possible girth  $g$ . The MPEG algorithm, suitable for design of rate-adaptive LDPC codes for optical communication applications, can be formulated as follows: Given  $(n - k)$  and bit-node degree distribution, design an  $(n - k) \times n$  parity-check matrix with girth  $g \geq 8$  and code rate  $R = k/n \geq 0.8$ . Before we fully describe the MPEG algorithm, we introduce several definitions that will facilitate its description. A *regular* LDPC( $n, k$ ) code is a linear block code whose parity-check matrix  $H$  contains exactly  $W_c$  1's per column and exactly  $W_r = W_c(n/(n - k))$  1's per row, where  $W_c \ll (n - k)$ . If  $H$  is low density, but the number of 1's per column or row is not constant, the corresponding code is an *irregular* LDPC code. Decoding of LDPC codes is based on sum-product algorithm (SPA), which is an iterative decoding algorithm where extrinsic probabilities are iterated back and forth between variable and check nodes of bipartite (Tanner) graph representation of a parity-check matrix  $H$ . The Tanner graph of an LDPC code is drawn according to the following rule: Check node  $c$  is connected to variable node  $v$  whenever the element  $h_{cv}$  in  $H$  is a 1. The code description can also be done by the degree distribution polynomials  $\lambda(x)$  [ $\rho(x)$ ] for the  $v$ -node ( $c$ -node) by  $\lambda(x) = \sum_{d=1}^{d_v} \lambda_d x^{d-1}$  [ $\rho(x) = \sum_{d=1}^{d_c} \rho_d x^{d-1}$ ], where  $\lambda_d$  ( $\rho_d$ ) denotes the fraction of the edges that are connected to degree- $d$   $v$ -nodes ( $c$ -nodes), and  $d_v$  ( $d_c$ ) denotes the maximum  $v$ -node ( $c$ -node) degree. For the  $v_i$ -node, we define its neighborhood  $N(v_i)$  as the set of  $c$ -nodes connected to it. The neighborhood of  $v_i$ -node at depth  $t$  is denoted by  $N^{(t)}(v_i)$ , and the complement of  $N^{(t)}(v_i)$  (the set of  $c$ -nodes not connected to  $v_i$ -node) by  $\bar{N}^{(t)}(v_i)$ .

The MPEG algorithm can be described as follows.

**Initialization.** Set  $m = n - k$ , the target girth  $g_{tg}$ , the lowest tolerable girth  $g_l$ ,  $v$ -nodes degree distribution  $\{d(v_i)\}$ , the maximum number of iterations (denoted as # iter), and iterators  $i = j = 0$ . Set also  $g_i = g_{tg}$  and control parameter  $control = 0$ .

**While**  $g_i \geq g_l$

For every  $v_i$ -node iterate ( $i = i + 1$ ):

Step 1. If there is no  $c$ -node connected to  $v_i$ -node, create an edge between  $v_i$ -node and  $c_j$ -node of lowest degree under current state of node connections.

Step 2. If  $\text{degree}(v_i) < d(v_i)$ , expand a tree from  $v_i$  to depth  $t$  under the current state of nodes connection until  $\bar{N}^{(t)}(v_i) \neq \emptyset$  but  $\bar{N}^{(t+1)}(v_i) = \emptyset$  or the cardinality of  $N^{(t)}(v_i)$  ( $< m$ ) saturates, and then, we create an edge between  $v_i$ -node and  $c_j$ -node of lowest degree from  $\bar{N}^{(t)}(v_i)$ .

Stopping criteria. Repeat step 2 until  $\text{degree}(v_i) = d(v_i)$ .

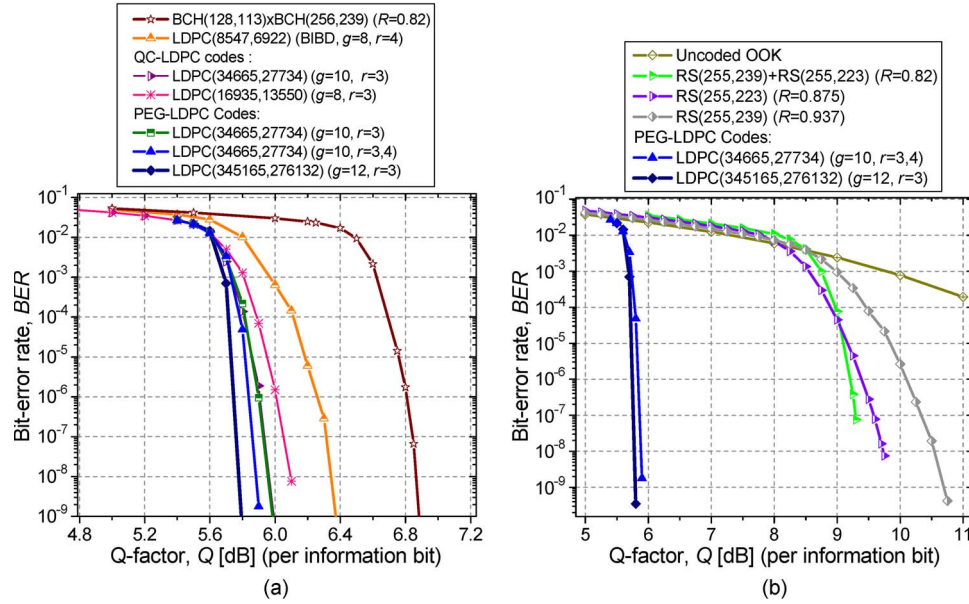


Fig. 3. BER performance of PEG-based LDPC codes. (a) PEG-LDPC codes against QC-LDPC codes and TPCs. (b) PEG-LDPC codes against RS and concatenated RS codes.

```

If  $g_i < g_{i-1}$ ,  $j < \# \text{ iter}$  and  $i == \text{control}$ 
    Delete all edges associated with  $v_i$  and  $v_{i-1}$  and reset  $i = i - 2$ ,  $j = j + 1$  and  $\text{control} = i$ 
End
If  $\text{control} == i$ 
    If  $g_i == g_{i-1}$  or  $j == \# \text{ iter}$ 
        Reset  $j = 0$ 
    End
End
End
Set the codeword length  $n$  to  $i - 1$ 

```

We now turn our attention to the BER performance evaluation of MPEG algorithm based LDPC codes. The results of simulations for the AWGN channel model are given in Fig. 3. In this figure, we compare the PEG-based LDPC codes against RS codes, concatenated RS codes, turbo-product codes (TPCs) [8], and QC-LDPC codes [6]. The PEG-based irregular LDPC(34665, 27734) code outperforms, observed at BER of  $10^{-9}$ , TPC of similar length [BCH(128, 113) × BCH(256, 239)] by 1 dB, and QC-LDPC(16935, 13550) code [6] by 0.2 dB. In addition to coding gain improvement, which can be considered small when compared with QC-LDPC codes, MPEG-based LDPC codes can push down the error floor of QC codes and offer much more flexibility in designing LDPC codes with desired code rate and length. Moreover, with MPEG algorithm we can design large-girth LDPC codes of shorter lengths compared to QC code design. The PEG-based irregular LDPC(34665, 27734) code outperforms the concatenation RS(255, 239) + RS(255, 223) (of rate 0.82) by 3.45 dB, and RS(255, 239) by 4.8 dB, both at BER of  $10^{-9}$ . The net effective coding gain (NECG) for PEG-based irregular LDPC(34665, 27734) code at BER of  $10^{-9}$  is 9.66 dB. Expected NECG at BER of  $10^{-12}$  is 11.05 dB. By using longer MPEG-based LDPC(345165, 276132) code, the NECG at BER of  $10^{-12}$  can be improved to 11.15 dB. We further designed a rate-adaptive MPEG-LDPC code of codeword length 16935 with possible code rates  $\{0.9, 0.875, 0.85, 0.8, 0.75, 0.7\}$ , whose BER performance is shown in Fig. 4.

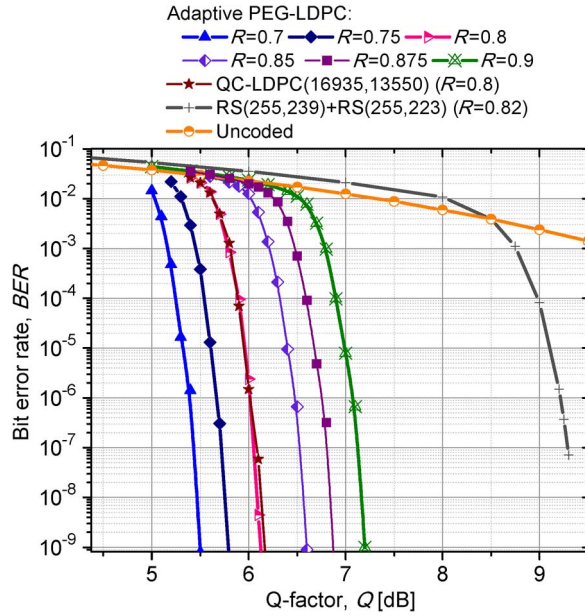


Fig. 4. BER performance of adaptive MPEG-LDPC codes.

#### 4. Adaptive MPEG-LDPC-Coded OFDM for Heterogeneous Access Optical Networks

In this paper, we propose the use of adaptive “water-filling” algorithm [9] as a means to deal with limited bandwidth of POF/MMF and OWC links. This algorithm is used to determine the optimum power to be allocated to the  $i$ th subcarrier  $P_i$  as follows:

$$P_i/P = \begin{cases} 1/\gamma_{\text{tsh}} - 1/\gamma_i, & \gamma_i \geq \gamma_{\text{tsh}} \\ 0, & \text{otherwise.} \end{cases} \quad (1)$$

In (1),  $P$  denotes the total available power, and  $\gamma_i$  denotes the SNR in the  $i$ th subcarrier. This SNR is defined as  $\gamma_i = |H[i]|^2 P/N_0$ , where  $H[i] = H_{\text{POF}}[i]H_{\text{OWC}}[i]$  denotes the transfer function of the  $i$ th subcarrier obtained by the product of the transfer functions of POF,  $H_{\text{POF}}[i]$  (as defined by Yabre [10]), and OWC links  $H_{\text{OWC}}[i]$ .  $N_0$  denotes the power spectral density of the receiver electronics noise. The optimum threshold SNR is determined from the condition that total power in all subcarriers cannot be larger than available power,  $\sum_i P_i \leq P$ , by the quick converging iterative procedure

$$\gamma_{\text{tsh}} = N / \left[ 1 + \sum_{i:\gamma_i > \gamma_{\text{tsh}}} 1/\gamma_i \right]. \quad (2)$$

In (2),  $N$  is the number of subcarriers with  $\gamma_i \geq \gamma_{\text{tsh}}$ . To deal with atmospheric turbulence we propose the use of spatial diversity principle. We show later in the text that using two photodetectors and EGC is sufficient to compensate for strong atmospheric turbulence. The corresponding channel capacity, which is defined as the maximum information rate that can be reliably transmitted over proposed heterogeneous optical communication system, is derived to be

$$C = E_l \left[ \sum_{i:\gamma_i > \gamma_{\text{tsh}}} B_{\text{sc}} \log_2 (l^2 \gamma_i / \gamma_{\text{tsh}}) \right] \quad (3)$$

where  $B_{\text{sc}}$  is the bandwidth of subcarrier channel,  $l$  is the irradiance of FSO channel, and  $E_l[\ ]$  denotes the expectation operator with respect to  $l$ . The variable-rate adaptation can be achieved by

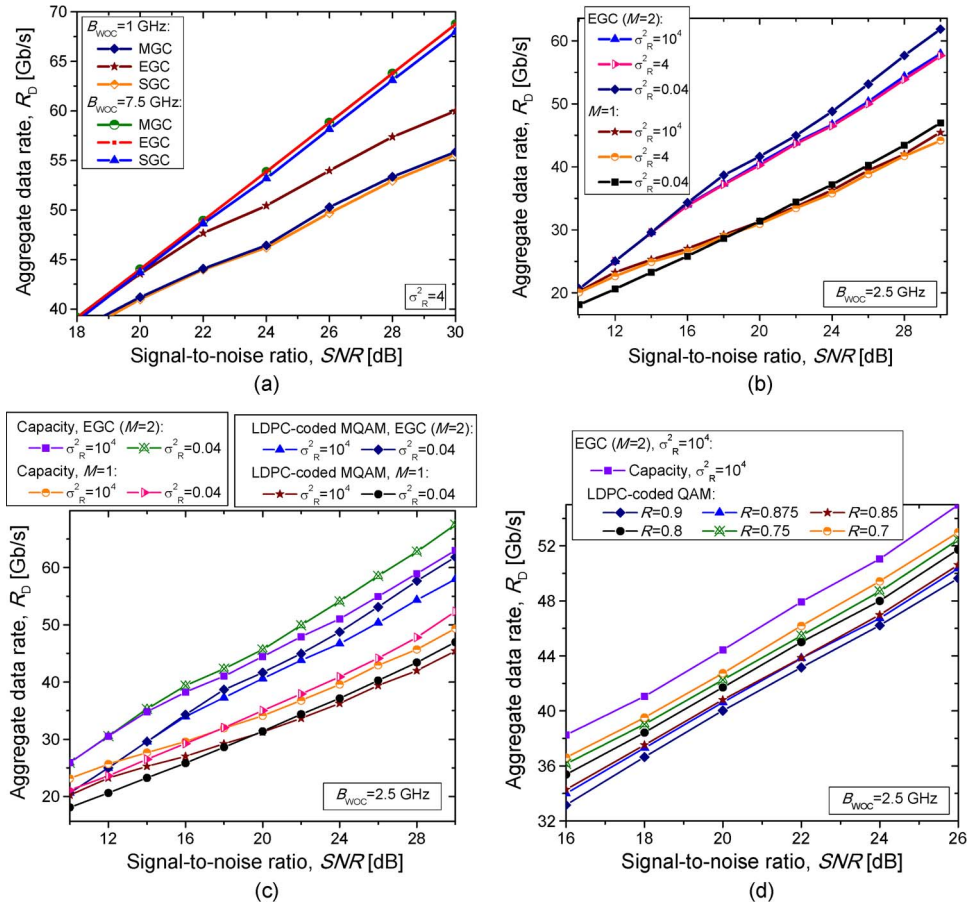


Fig. 5. Aggregate data rates of heterogeneous access optical communication system at BER of  $10^{-9}$  for LDPC code of rate  $R = 0.875$  (a) for different FSO spatial diversity scenarios under the strong turbulence regime, (b) for various atmospheric turbulence regimes, (c) channel capacity derived aggregate data rates against LDPC-coded OFDM ( $R = 0.875$ ), and (d) aggregate data rates in saturation regime for various code rates.

choosing the maximum product of integer  $m_i$ , corresponding to the number of bits per  $i$ th subcarrier, and code rate  $R$  of corresponding LDPC code as follows:

$$m_i R \leq \log_2(\gamma_i / \gamma_{tsh}) = C_i. \tag{4}$$

In (4),  $C_i$  [bits/channel use] denotes the channel capacity of the  $i$ th subcarrier. The rate-adaptive LDPC code is designed as described in previous section. The uniformly generated sequence is LDPC encoded and the output of encoder is written into a buffer. The  $m_i$  bits (for  $i$ th subcarrier) are taken from the buffer and used as input to the mapper. The QAM signal constellation size  $2^{m_i}$  per  $i$ th subcarrier and the corresponding code rate  $R$  of LDPC code are chosen in accordance with the subcarrier SNR. When the subcarrier SNR  $\gamma_i$  is high, larger constellation size is employed. When  $\gamma_i$  is low, we reduce the signal constellation size according to Eq. (4), and do not transmit at all on subcarriers with subcarrier SNR below threshold  $\gamma_{tsh}$ . The OFDM receiver processing and LDPC decoding is similar to that already reported in [1] and [6]. Different LDPC codewords are transmitted over the heterogeneous channel until 1000 bit errors are counted or  $10^9$  codewords are transmitted, whichever is shorter.

Fig. 5 shows the channel capacities and spectral efficiencies of the proposed heterogeneous FSO-POF-OWC system, corresponding to OFDM signal bandwidth of 7.5 GHz with 128 subcarriers. (Correspondence is based on the bandwidth of UWB signal.) We report the corresponding plots for

100 m of GIPOF50 (from Thorlabs) at 1330 nm (of suboptimum exponent index  $g = 2.1$ ) and for different FSO turbulence strengths. The atmospheric turbulence strength is characterized by Rytov variance [1]  $\sigma_R^2 = 1.23 C_n^2 k^{7/6} L^{11/6}$ , where  $k = 2\pi/\lambda$  denotes the wavenumber ( $\lambda$  is the wavelength),  $L$  denotes the propagation distance, and  $C_n^2$  is the refractive index structure parameter. Weak fluctuations are associated with  $\sigma_R^2 < 1$ , strong with  $\sigma_R^2 > 1$ , and the saturation regime is specified by  $\sigma_R^2 \rightarrow \infty$ .

The OWC link typically contains the line-of-sight (LOS) and diffuse components. In Fig. 5, we observe the worst case scenario, that is only diffuse component is present [see Fig. 1(c)]. The diffuse component is commonly modeled as the low-pass filter [1] of bandwidth  $B_{\text{OWC}}$ . To model the propagation of signal over the POF links, we employ a comprehensive model due to Yabre [10]. This model includes mode coupling and mode attenuation. We see that beyond 40-Gb/s transmission over proposed heterogeneous optical system is possible for  $M = 2$  FSO receivers and EGC at moderate SNRs. To concentrate on channel distortions only, we assumed that MZM, LD and SLD/VCSEL modulation characteristics are ideal. In Fig. 5(a), we provide the aggregate data rates for various FSO spatial diversity techniques (MGC, EGC, and SGC) under the strong turbulence regime ( $\sigma_R^2 = 4$ ). For sufficient OWC link bandwidth MGC and EGC perform comparable and slightly outperform SGC. However, when OWC link bandwidth is significantly lower than OFDM signal bandwidth the EGC is much robust compared to MGC. In simulations, we employ no optical amplifier; therefore, the major contributor to noise effects is thermal noise of transimpedance amplifier in the final receiver stage. The SNR in Fig. 5 is, therefore, defined in the electrical domain upon photodetection in last receiver stage. In Fig. 5(b), we provide a comparison between a single FSO receiver and an EGC with  $M = 2$  FSO receivers for various turbulence regimes for a fixed OWC link bandwidth of  $B_{\text{OWC}} = 2.5$  GHz. For EGC and  $M = 2$  FSO receivers, the aggregate data rate of 40 Gb/s can be achieved at medium SNRs, while for a single FSO receiver, it can only be achieved for high SNR values. It is interesting to notice that communication, even in the FSO saturation regime, is possible with the proposed scheme. In Fig. 5(c), we compare the channel-capacity-derived aggregate data rates against LDPC-coded OFDM with QAM. For an aggregate data rate of 40 Gb/s under saturation regime when two FSO receivers are used and EGC, we are 2.27 dB away from channel capacity when the LDPC, code of rate 0.875 is used. Finally, in Fig. 5(d), we compare the aggregate data rates under saturation regime for various code rates. When an LDPC code of rate 0.75 is used, for an aggregate rate of 40 Gb/s, we are 1.33 dB away from channel capacity, while for the  $R = 0.7$  code, we are only 1.04 dB away from channel capacity.

## 5. Conclusion

In this paper, the heterogeneous access optical networking scenario, composed of heterogeneous FSO-POF-OWC links, is proposed, which can deliver the data rates of 40 Gb/s and beyond to an end-user. The proposed scheme employs power-variable rate-adaptive LDPC-coded OFDM to deal with bandwidth limitations of POF/MMF and OWC links and the spatial diversity to deal with the atmospheric turbulence. The rate-adaptive LDPC codes are designed using the MPEG algorithm introduced here. The proposed scheme can operate even in the saturation atmospheric turbulence regime. The proposed heterogeneous FSO-POF-OWC system has many advantages compared with PONs and RoF systems: i) enabling ultrahigh-speed transmission to end-users, ii) allowing interoperability of various RF and optical technologies, iii) reducing installation costs, iv) reducing deployment time, and v) improving the energy efficiency of heterogeneous communication link.

## References

- [1] W. Shieh and I. Djordjevic, *OFDM for Optical Communications*. Amsterdam, The Netherlands: Elsevier, 2009.
- [2] A. Stöhr, A. Akrouf, R. Bu, B. Charbonnier, F. van Dijk, A. Enard, S. Fedderwitz, D. Jäger, M. Huchard, F. Lecoche, J. Marti, R. Sambaraju, A. Steffan, A. Umbach, and M. Wei, "60 GHz radio-over-fiber technologies for broadband wireless services," *OSA J. Opt. Netw.*, vol. 8, no. 5, pp. 471–487, May 2009.
- [3] M. Ghavami, L. B. Michael, and R. Kohno, *Ultra Wideband Signals and Systems in Communication Engineering*. New York: Wiley, 2007.

- [4] C. F. Lam, *Passive Optical Networks: Principles and Practice*. Amsterdam, The Netherlands: Elsevier, 2007.
- [5] X.-Y. Hu, E. Eleftheriou, and D. M. Arnold, "Regular and irregular progressive edge-growth Tanner graphs," *IEEE Trans. Inf. Theory*, vol. 51, no. 1, pp. 386–398, Jan. 2005.
- [6] I. B. Djordjevic, W. Ryan, and B. Vasic, *Coding for Optical Channels*. New York: Springer-Verlag, 2010.
- [7] M. P. C. Fossorier, "Quasi-cyclic low-density parity-check codes from circulant permutation matrices," *IEEE Trans. Inf. Theory*, vol. 50, no. 8, pp. 1788–1794, Aug. 2004.
- [8] T. Mizuochi, Y. Miyata, T. Kobayashi, K. Ouchi, K. Kuno, K. Kubo, K. Shimizu, H. Tagami, H. Yoshida, H. Fujita, M. Akita, and K. Motoshima, "Forward error correction based on block turbo code with 3-bit soft decision for 10-Gb/s optical communication systems," *IEEE J. Sel. Topics Quantum Electron.*, vol. 10, no. 2, pp. 376–386, Mar./Apr. 2004.
- [9] T. M. Cover and J. A. Thomas, *Elements of Information Theory*. New York: Wiley, 1991.
- [10] G. Yabre, "Theoretical investigation on the dispersion of graded-index polymer optical fibers," *J. Lightwave Technol.*, vol. 18, no. 6, pp. 869–877, Jun. 2000.